Optogalvanic spectroscopy with microplasma sources – Current status and development towards a lab on a chip

Anders Persson[1,2], Martin Berglund[1,2], Zahra Khaji[1], Peter Sturesson[1, 2, 3], Johan Söderberg[1,2], Greger Thornell[1,2]

[1]Uppsala University; Division of Microsystems Technology, Uppsala, Sweden

[2]Uppsala University; Ångström Space Technology Centre, Uppsala, Sweden

[3]Swedish Defence University, Div. of Military Technology, Dep. of Military Sciences, Stockholm, Sweden

E-mail: anders.persson@angstrom.uu.se

This document is the Post-print version of a Published Work that appeared in final form in Journal of Micromechanics and Microengineering. To access the final edited and published work see: http://iopscience.iop.org/journal/0960-1317.

Abstract. Miniaturized optogalvanic spectroscopy shows excellent prospects of becoming a highly sensitive method for gas analysis in micro total analysis systems. Here, a status report on the current development of microwave induced microplasma sources for optogalvanic spectroscopy is presented, together with the first comparison of the sensitivity of the method to conventional single-pass absorption spectroscopy. The studied microplasma sources are stripline split-ring resonators, with typical ring radii between 3.5 and 6 mm and operation frequencies around 2.6 GHz. A linear response (R^2=0.9999), and a stability of more than 100 s are demonstrated when using the microplasma source as an optogalvanic detector. Additionally, saturation effects at laser powers higher than 100 mW are observed, and the temporal response of the plasma to periodic laser perturbation with repletion rates between 20 Hz and 200 Hz are studied. Finally, the potential of integrating additional functionality with the detector is discussed, with the particular focus on a pressure sensor and a miniaturized combustor to allow for studies of solid samples.

1. Introduction

Optogalvanic spectroscopy (OGS) is the study of atomic and molecular transitions in the ultraviolet, visible and infrared (IR) regimes using the so called optogalvanic effect (OGE) [1]. This effect describes the interaction between an atomic or molecular gas discharge, or plasma, and resonant radiation, typically in the form of a laser beam. When irradiated, the gas absorbs photons at transitions resonant with the laser frequency. This can have one of several effects on the discharge or plasma, where, e.g., an excited atomic state can either favor or inhibit ionization, hence affecting the electron and ion densities in the plasma. If the absorption instead causes the excitation of a higher order rotational or vibrational state in a molecule, collisional de-excitation will affect the temperature of the different plasma species, and hence the electron mobility. Although different in nature, both these processes will affect the impedance of the discharge, which, in one way or another, is the entity measured in OGS.

OGS was a hot topic in the 1970s and 80s [2–4], but failed to address any lasting applications apart from being used to study metal ions in hollow cathode discharge tubes [2, 3]. However, with the recent advent of tunable, narrow line-width solid-state lasers such as interband and quantum cascade lasers [7], IR OGS has started to gain momentum, and has been proposed for applications in as diverse fields as planetary exploration, greenhouse gas monitoring and life science [5-7].

One of the major advantages with OGS is that it scales well with miniaturization. Whereas the signal strength in ordinary absorption spectroscopy is linearly dependent on the interaction length between the laser beam and the sample gas, meaning that a smaller instrument inherently will be able to extract less signal from the sample, the signal generation in OGS is fundamentally different and less dependent on the volume of the sample cell [1]. Particularly interesting in this respect are OGS systems that employ Langmuir probes to measure the signal. These only rely on the fraction of sample gas that is present in the sheet of the probe to generate the signal. From this miniscule volume, OGS can extract orders of magnitude stronger signal than an absorption spectrometer [11]. Hence, the OGE in combination with a microplasma source offers a very interesting case for highly miniaturized IR spectroscopy, and can develop into a very promising measurement technique for future micro total analysis systems (μTAS) and lab on a chip (LOC).

During the last couple of years, we have studied such a system employing a stripline split-ring resonator (SSRR) as a plasma source [6-7, 9-10]. Here, we report on the latest progress in this endeavor, investigate saturation effects and response times in the plasma, study the linearity of the method, and present a first comparison between the sensitivity of our system and single-pass absorption spectroscopy.

2. Theory

The theory of OGS is more complicated than that of, e.g, absorption spectroscopy, since the presence of a plasma adds several additional variables, primarily the energy and density of the electrons and ions.

We have put substantial efforts into developing theory for the OGE in a microwave plasma when it is biased to a potential above the equilibrium plasma potential by one of two Langmuir probes [9]. In such a configuration, the optogalvanic signal is measured as a perturbation of the floating potential of the other probe, and it has been shown that both the amplitude and stability of the signal improves rapidly as the bias voltage is increased, up to a point where the biased probe starts to quench the plasma. In this configuration, the optogalvanic signal, U_{OG}, can be approximated by:

$$U_{\mathrm{OG}} = \pi l r^2 n_{\mathrm{m}} I_0 \sigma_{\mathrm{L}} \frac{eK}{k_{\mathrm{B}} T_{\mathrm{e}}} U_{\mathrm{F}} \,, \tag{1}$$

where U_{F} is the floating potential of the unbiased probe, $\pi l r^2$ is the cylindrical volume of the plasma subjected to a laser beam with intensity I_0, σ_{L} is the absorption cross section of the photon-molecule interaction, n_{m} is the volume density of excitable molecules, T_{e} is the electron temperature, k_{B} is Boltzmann's constant, e is the charge of an electron, and K is a proportionality constant unique to each transition.

Still, this equation should be regarded as a first order approximation, since several other processes too affect the signal, e.g., collisional excitation of higher order rovibrational states in the molecules [9]. Hence, thorough monitoring of the plasma is required in order to understand its dynamics, and to be able to apply the OGE to spectrometric applications.

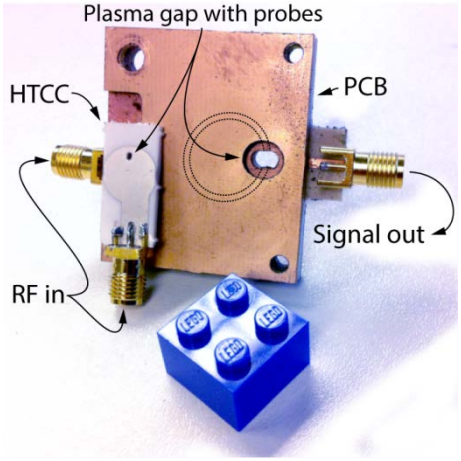

Figure 1. Photograph of the two SSRR designs. The dotted lines show the approximate position of the split-ring resonator in the PCB plasma source. In front of this device, aligned to its lower, left corner is the newer, ceramic device. A Lego brick (16 x 16 x 11.4 mm in size) has been added as a reference.

3. Devices and systems

Through the years, we have employed several different designs, materials and fabrication methods when making our split-ring resonator plasma sources [8–10,12–14]. For example, both microstrip and stripline waveguides have been fabricated on, e.g., silicon and Pyrex, using standard MST processes such as sputtering, electroplating, and wet and reactive ion etching. We now focus on two systems based on milling and bonding of either printed circuit board (PCB) or high-temperature co-fired ceramic (HTCC) alumina, figure 1, employing copper or platinum as conductive material. Moreover, both systems utilize a stripline configuration to improve the electromagnetic compatibility (EMC). The fabrication of PCB and HTCC SSRRs are thoroughly described in [13] and [14], respectively.

The two types of devices have ring radii between 3.5 and 6 mm, operate at frequencies around 2.6 GHz, and generally require less than 1 W to maintain the plasma. The width of the gap through the ring has been varied between 0.5 and 5 mm, and the interaction length between the laser beam and the sample, i.e. the path length, is typically less than 5 mm.

The SSRRs have been tested in several configurations. For example, the EMC of the stripline concept has been evaluated by the Wheeler cap method [13], and the dielectric properties of HTCC alumina have been charted at frequencies around 2.6 GHz [14]. Different ways of integrating Langmuir probes in the SSRR have also been investigated [15]. These probes have been made from 25 µm in diameter gold or platinum bond wires and are used to analyze the plasma, and, more importantly, extracting the optogalvanic signal from the detector.

However, most important have been the optogalvanic experiments that have investigated the ability of the SSRR detectors to properly measure the OGE in the microwave plasma. A typical setup for such experiments is shown in figure 2. The three principal parts of the setup are the optical, fluidic and electrical systems. The optical system has this far relied on tunable, single-mode CO_2 lasers to excite the plasma. The current setup includes two such lasers, one with $^{12}CO_2$ and one with $^{13}CO_2$ wavelengths. A third HeNe laser is used to align the IR lasers to the plasma source. Moreover, only single-pass systems have been investigated, although multi-pass systems and optical cavities have been proposed for future studies [9]. In this paper, we present results obtained using the $^{12}CO_2$ laser, more precisely a Merit SL laser from Access Lasers Inc.

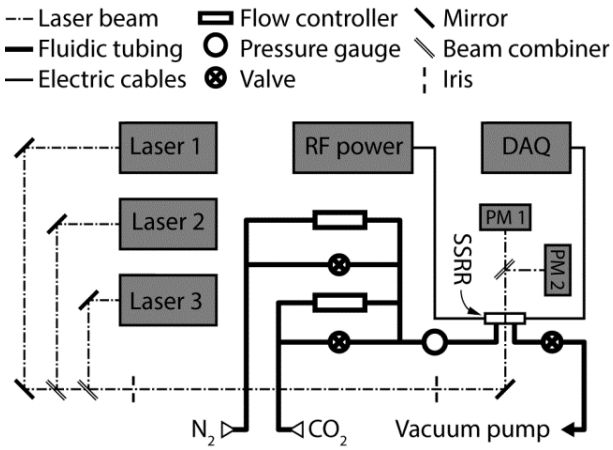

Figure 2. Schematics of the OGS setup with optics, fluidics and electronics. PM denotes (laser) power meter, and DAQ data acquisition unit.

Because of the CO_2 lasers, the experiments have focused at spectroscopic studies of pure CO_2 or mixtures of CO_2 and N_2. Moreover, the experiments have been conducted at pressures in the 10 to 1000 Pa range with ([12]) or without ([5-7]) a flow through the SSRR. In this paper, results from both configurations are presented.

Finally, the electronics consists of an RF power supply with tunable frequency and amplification, and a signal detection system, in its simplest form only consisting of an analog-input data acquisition (DAQ) unit [8], but with the optional addition of a source meter for applying a constant bias voltage to one of the Langmuir probes [6, 9], and/or – as presented here – a lock-in amplifier.

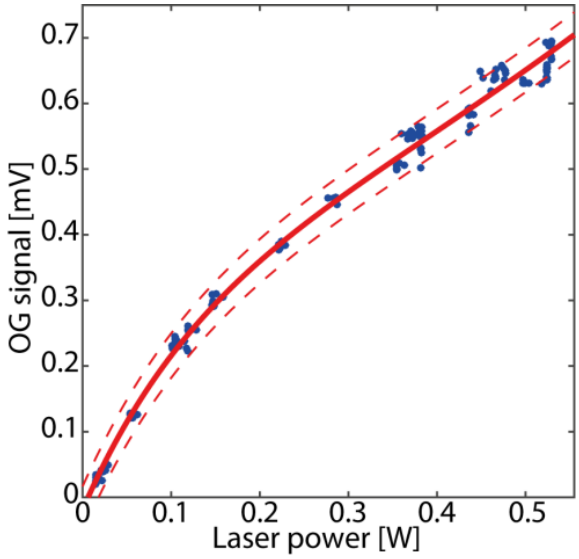

Figure 3. Optogalvanic signal as a function of laser power in a 150 Pa CO_2 plasma. The solid line shows an exponential fit to the measurement, and the dashed lines show a 95% confidence interval.

4. Measurements, results and discussion

This far, most of our efforts have been directed towards either improving the SSRR [7, 10-12] or furthering the understanding of the OGE in a microwave plasma [5, 6]. In this paper, we now explore the spectroscopic performance of the system and compare it with standard absorption spectroscopy. Some important properties in such a comparison are saturation effects and response times in the plasma, the spectral resolution of the measurement, and the stability and reproducibility of the signal.

With respect to saturation, figure 3 shows the dependency of the optogalvanic signal on the laser power. From literature [1] it is known that the signal commonly saturates at high laser power (or high

sample concentrations), and figure 3 displays signs of saturation at powers above ~100 mW. From preliminary experiments, we found that even higher laser powers (>1 W) caused continued saturation. However, the saturation behavior of the optogalvanic signal is likely to depend on several other parameters such as the pressure, temperature and composition of the gas, and should be evaluated separately for each experiment. Still, over small power intervals, the optogalvanic signal depended more or less linearly on the laser power, enabling spectrometric measurements.

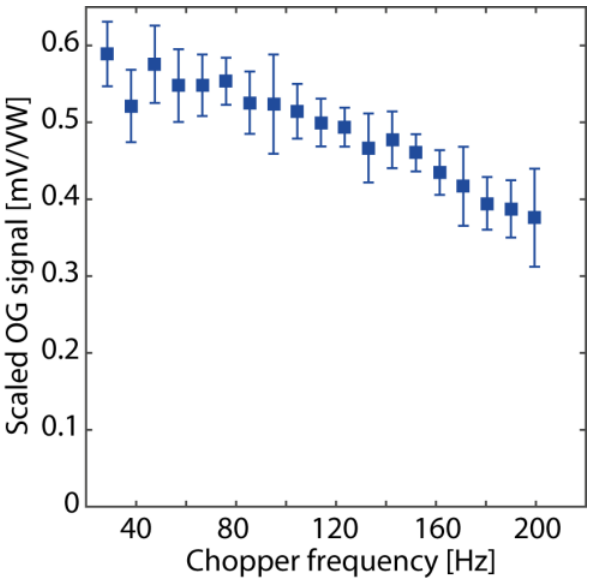

Figure 4. Optogalvanic signal scaled by the probe potential and laser power as a function of chopper frequency in a 150 Pa CO_2 plasma.

With respect to response time, i.e., the ability of the plasma to respond to laser pulses of different modulation frequencies, the interaction between the laser beam and the plasma must be investigated in more detail. Figure 4 shows the dependency of the optogalvanic signal on the modulation frequency of the laser beam. A signal reduction of about 25% was observed going from 20 Hz to 200 Hz, which was likely explained by the different time scales of the major absorption and deactivation processes in the plasma.

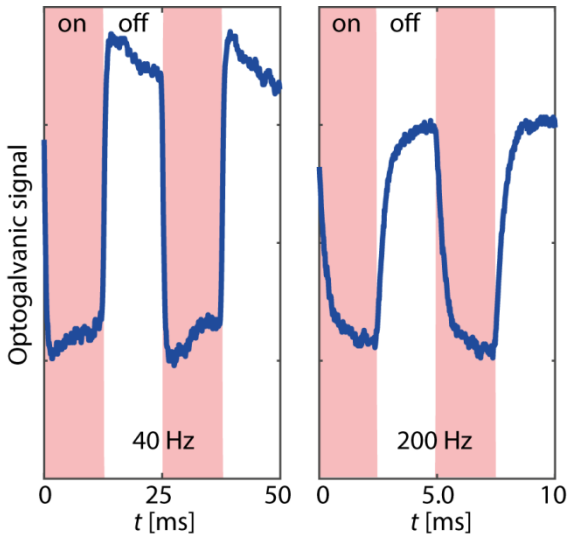

Figure 5. Optogalvanic signal as a function of time in a 150 Pa CO_2 plasma, for a chopper frequency of 40 Hz (left) and 200 Hz (right). The colored background shows the laser on and off states.

In the experiment behind figure 4, the laser was stabilized at the P20 transition of the CO_2 laser, i.e., at a wavelength of 10.6 µm [10]. The most important optical absorption process for such photons in a pure CO_2 plasma is the excitation of sample molecules from the first symmetric to the first asymmetric stretch mode, i.e. from the (100) to the (001) level [16]. This excitation causes a depletion of the (100) level, which is repopulated by either deactivation from the (001) level or by thermal activation from the ground state (000). These processes either heat or cool the plasma, and both have rate constants in the 200-400 s^{-1} range at pressures relevant to our experiments. The measured waveforms, figure 5 (right), show great agreement with theoretical predictions [17], and indicate cooling as the principal mechanism, suggesting that the repopulation of the (100) level is the main process driving the generation of the optogalvanic signal in the pure CO_2 plasma.

Waveforms at lower frequencies showed an additional, much slower, heating component, figure 5 (left). It is unclear if this component is spectroscopic in origin, or, e.g., a result of thermal interaction between the laser beam and the device itself. If so, the apparent increase of the signal amplitude at lower frequencies in figure 4 is not optogalvanic in origin, but merely an increasing background. However, this effect needs to be investigated in more detail before any firm conclusions can be drawn.

With respect to resolution, figure 6 shows a measurement of pure CO_2 at 500 Pa, where the cavity length of the gratingless laser was tuned across the voltage range of the piezoelectric position control of its back mirror. This produced an output with a wavelength varying over a total of seven $^{12}CO_2$ P-lines in the 10.5-10.7 µm range as verified with a spectrum analyzer.

Figure 6 shows that the SSRR detector could detect and separate the different lines with good resolution. For the first time in our experiments, a lock-in amplifier was used for the detection, and given the promising results – especially with respect to signal-to-noise ratio (SNR) – this approach will be investigated further in future experiments.

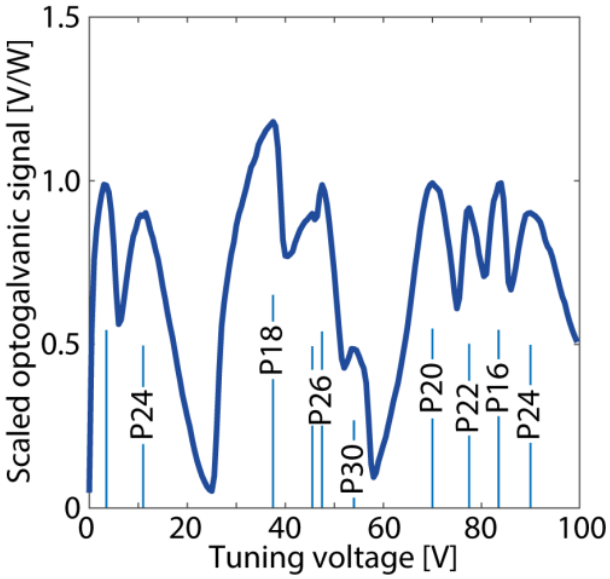

Figure 6. Optogalvanic spectrum over several CO_2 lines in a 500 Pa CO_2 plasma. The optogalvanic signal has been scaled by the laser power.

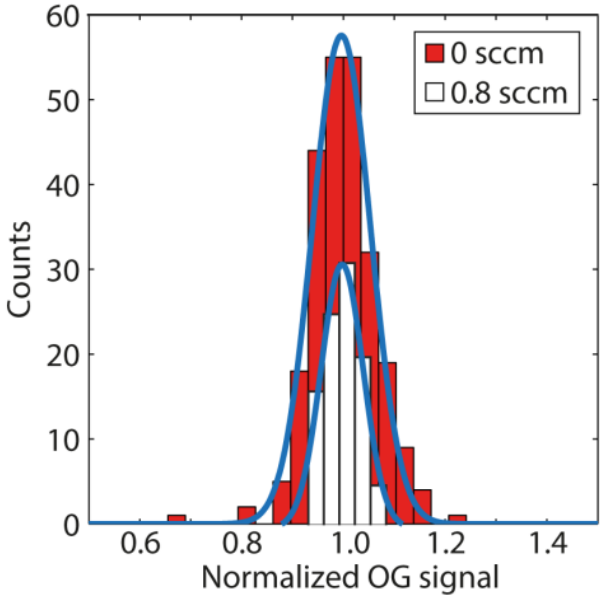

Figure 7. Measurement precision in five different measurements with 50 data points each, with or without a flow through the plasma source.

With respect to reproducibility, figure 7 shows a comparison of the precision when the sample is either flowed through the plasma at a constant rate or kept static, i.e. zero flow. The experiments each consisted of a total of five identical measurements on identical samples, although the pressure in the experiment with flow was lower than in that without, and the gas mixtures also were somewhat different. The individual measurements were conducted at different times over a period of three days, where the setup was completely re-initialized between each measurement. The figure shows the distribution of the individual data points after having been normalized to the common average, i.e., the average of all the experiments combined. As can be seen, both experiments showed Gaussian distribution fits, suggesting good reproducibility.

Although the difference in the experiments (pressure, gas mixture, etc.) could be responsible for some of the observed differences in precision, the results presented in figure 7 are indicative of all our experiments with and without flow, where the former consistently generated better reproducibility than the latter. In figure 7, the full-width-at half-maximum was about 20% more narrow with flow than without. Moreover, in measurements without flow, the reproducibility improved as the size of the instrument was reduced [10]. Hence, reproducibility was favored by miniaturization, probably due to the plasma reaching chemical equilibrium more rapidly in a smaller cell, and the reproducibility in both experiments behind figure 7 was an order of magnitude better than what is usually accomplishable with a macroscopic plasma source [18].

With regards to stability, figure 8 shows the Allan deviation of a typical measurement after both the laser and the plasma had stabilized [10]. The Allan deviation is a measure of the frequency stability of a system, and can be used to characterize both noise processes and systematic errors such as drift. As can be seen, the signal was stable over time scales of up to 100 s, (turning point of the curve), which means that substantial averaging is possible to improve the SNR. Beyond 100 s drift in the signal will start to become apparent. In order to improve the stability, active frequency stabilization of the laser could be beneficial, indicating that the performance of the SSRR as an OGS detector still has considerable room for improvement.

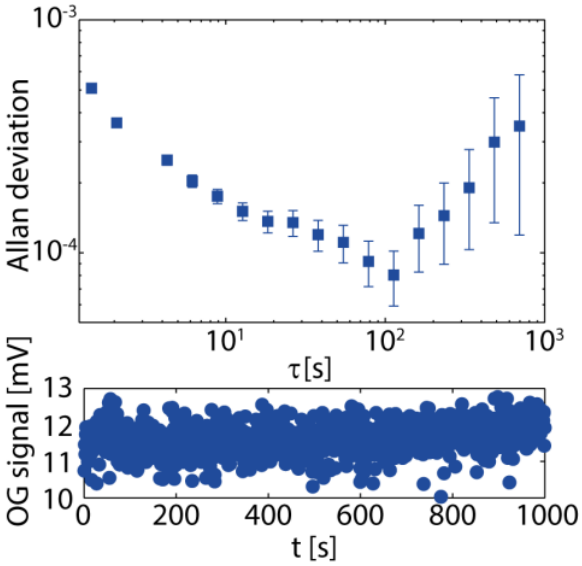

Figure 8. Typical Allan deviation of a measurement (top) with the corresponding time series (bottom).

Even though the system is far from optimized, it already performs very well compared to conventional IR spectroscopy. Figure 9 shows a comparison between OGS and single-pass absorption spectroscopy, where the signal difference between a measurement on pure N_2 and one where 225 ppm CO_2 has been added to the N_2 is shown. The pressure in both experiments was 300 Pa. As can be seen, the absorption detector could not distinguish the small amount of CO_2 from the N_2 background. The optogalvanic signal, on the other hand, was clearly distinguishable. Applying averaging and lock-in amplification to this experiment would enable measurements of the CO_2 concentration with good precision and accuracy. This demonstrates the capability of the SSRR detector to extract a strong signal from an extremely limited amount of sample. In the experiment presented in figure 9, the total amount of carbon inside the sample cell was in the picogram range, which correlates to, e.g., the carbon from a few dozen E. coli bacteria. Hence, it is reasonable to believe that SSRR OGS will become very competitive in applications where the total sample amount is inherently limited, for example in many LOC applications.

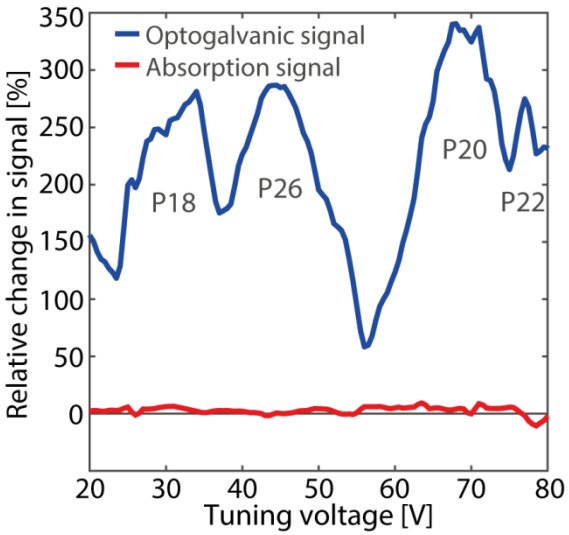

Figure 9. Relative signal change between measurements on pure N_2 and N_2 with 225 ppm CO_2 in a 5 mm long, single-pass sample cell. The pressure in both experiments was 300 Pa.

Equally promising are the results presented in figure 10, where the dependence of the OG signal on the concentration of CO_2 in N_2 is displayed. The results have been scaled using equation 1, and show that the OG signal depends more or less linearly (R^2=0.9999) on the CO_2 concentration in a range between

15.6 and 625 ppm. This does not only validate the theoretical framework, but also shows the prospects of using the detector for spectrometric experiments.

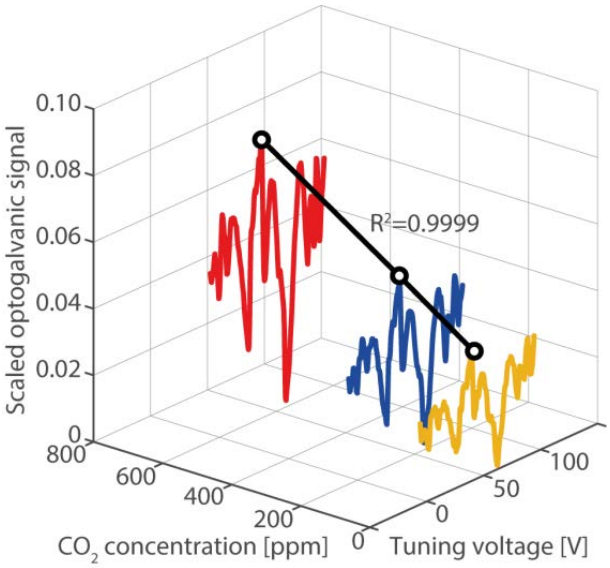

Figure 10. Spectrum of CO_2 diluted in N_2 at different concentrations (15.6, 225 and 625 ppm). The black line shows a linear fit to the P18 peak of the spectra.

However, in order to be able to analyze small samples properly, the detector has to be integrated with a microfluidic sample handling system. Based on this, the first steps towards integrating the SSRR with a micro-combustor [19] to enable the study of small, solid samples, are currently being taken in our laboratory. The combustor was made in HTCC alumina, and incorporates a 1 µl combustion chamber with an integrated heater and platinum temperature sensor. Using *in-situ* electroplating of copper followed by thermal oxidation, a copper oxide layer was added to the heater surface after sintering, to be used as a source of oxygen for combustion (oxidation) of solid samples at temperatures above 800 °C [20,21]. The amount of oxygen released by the copper oxide could be controlled by varying the thickness of the electroplated layer, where about 0.17 µmol of oxygen, corresponding to a thickness of 400 nm, was enough to combust up to 2 µg of carbon into CO_2. The function of the combustor has been verified by residual gas analysis, and the combustor will now be integrated with the SSRR.

Moreover, theory suggests that the OGE requires close monitoring of the plasma if it is to be used for spectrometry. Hence, sensors for measuring pressure, temperature (of electrons, ions and neutrals), and flow also need to be integrated into the system. For monitoring the gas pressure between the combustor and the SSRR, a microscale Pirani gauge with an integrated platinum bond-wire sensor element, has been developed [22]. Like the combustor, the pressure sensor was made in HTCC alumina, and consists of a separate cavity connected to the main gas flow channel. The bond wire is freely suspended through the cavity to, e.g., avoid thermal crosstalk with the bulk. The device has been shown to produce an exponential output in the 1.5 to 16 Torr (200 to 2100 Pa) range, exhibiting a sensitivity of about 0.36_Ω/$\log_{10}$Torr. Here, the signal from the sensor was defined as the change in resistance of the wire when powered with a 109 mA (rms), 1 kHz sine wave.

5. Conclusion

The ongoing work on developing a spectrometer using an SSRR microplasma source detector for OGS is reaching a point where actual benchmarking with other spectroscopic techniques can commence. In this paper, a comparison between OGS and single-pass absorption spectroscopy showed that the former technique could measure a clear signal well below the detection limit of the latter. Moreover, a linear response in the 100 ppm range (R^2=0.9999) was demonstrated, along with a stability of more than 100 s, and good reproducibility, especially in experiments where the sample was flowed through

the detector. Building on these results, we now focus our efforts on turning the SSRR spectrometer into a full LOC device.

Acknowledgements
The authors would like to acknowledge the Swedish National Space Board for funding the project.

References

[1] Barbieri B, Beverini N and Sasso A 1990 Optogalvanic spectroscopy *Rev. Mod. Phys.* **62** 603–44
[2] Schneck P K and Hastie J W 1981 Optogalvanic Spectroscopy-Application To Combustion Systems *Opt. Eng.* **20** 204522–204522 –
[3] Walkup R, Dreyfus R W and Avouris P 1983 Laser Optogalvanic Detection of Molecular Ions *Phys. Rev. Lett.* **50** 1846–9
[4] Webster C R and Menzies R T 1983 Infrared laser optogalvanic spectroscopy of molecules *J. Chem. Phys.* **78**
[5] Cavasso-Filho R L, Mirage A, Scalabrin A, Pereira D and Cruz F C 2001 Laser spectroscopy of calcium in hollow-cathode discharges *J. Opt. Soc. Am. B* **18** 1922–7
[6] Windholz I S and S K and B G and J D and L 2013 Optogalvanic spectroscopy of the hyperfine structure of weak La I lines: discovery of new even parity fine structure levels *J. Phys. B At. Mol. Opt. Phys.* **46** 65002
[7] Risby T H and Tittel F K 2010 Current status of midinfrared quantum and interband cascade lasers for clinical breath analysis *Opt. Eng.* **49** 111114–23
[8] Berglund M, Thornell G and Persson A 2013 Microplasma source for optogalvanic spectroscopy of nanogram samples *J. Appl. Phys.* **114** 33302
[9] Persson A, Berglund M and Salehpour M 2014 Improved optogalvanic detection with voltage biased Langmuir probes *J. Appl. Phys.* **116** 243301
[10] Persson A, Berglund M, Thornell G, Possnert G and Salehpour M 2014 Stripline split-ring resonator with integrated optogalvanic sample cell *Laser Phys. Lett.* **11** 45701
[11] Suzuki T, Sekiguchi H and Kasuya T 1983 OPTOGALVANIC DETECTION WITH MICROWAVE DISCHARGE *J. Phys. Colloq.* **44** C7–419 – C7–427
[12] Persson A and Salehpour M 2015 Intracavity optogalvanic spectroscopy: Is there any evidence of a radiocarbon signal? *Nucl. Instruments Methods Phys. Res. Sect. B Beam Interact. with Mater. Atoms* **361** 8–12
[13] Berglund M, Grudén M, Thornell G and Persson A 2013 Evaluation of a microplasma source based on a stripline split-ring resonator *Plasma Sources Sci. Technol.* **22** 55017
[14] Berglund M, Persson A and Thornell G 2015 Evaluation of dielectric properties of HTCC alumina for realization of plasma sources *J. Electron. Mater.* **44** 3654–60
[15] Berglund M, Sturesson P, Thornell G and Persson A 2015 Manufacturing miniature Langmuir probes by fusing platinum bond wires *J. Micromechanics Microengineering* **25** 105012
[16] Eilers G, Persson A, Gustavsson C, Ryderfors L, Mukhtar E, Possnert G and Salehpour M 2013 The radiocarbon intracavity optogalvanic spectroscopy setup at Uppsala *Radiocarbon* **55** 237–50
[17] Liakhou G, Paoloni S and Bertolotti M 2004 Observations of laser cooling by resonant energy transfer in CO_2–N_2 mixtures *J. Appl. Phys.* **96** 4219–24
[18] Persson A, Eilers G, Ryderfors L, Mukhtar E, Possnert G and Salehpour M 2013 Evaluation of intracavity optogalvanic spectroscopy for radiocarbon measurements *Anal. Chem.* **85** 6790–8
[19] Khaji Z, Sturesson P, Klintberg L, Hjort K and Thornell G 2015 Manufacturing and characterization of a ceramic microcombustor with integrated oxygen storage and release element *J. Micromechanics Microengineering* **25** 104006
[20] Khaji Z, Sturesson P, Hjort K, Klintberg L and Thornell G 2014 Investigation of the storage and release of oxygen in a Cu-Pt element of a high-temperature microcombustor *J. Phys. Conf. Ser.* **557** 12078
[21] Merritt D A, Freeman K H, Ricci M P, Studley S A and Hayes J M 1995 Performance and Optimization of a Combustion Interface for Isotope Ratio Monitoring Gas Chromatography/Mass Spectrometry *Anal. Chem.* **67** 2461–73

[22] Söderberg Breivik J 2015 Microscale Ceramic Pressure Sensor Element for a Carbon Isotope Analysis System for Planetary Exploration : Design, Manufacturing and Characterization. UPTEC Q15004, Uppsala (urn:nbn:se:uu:diva-257533).